

Characterization of dispersion in an alluvial aquifer by tracing techniques and stochastic modelling

N. COURTOIS*, O. GERBAUX-FRANCOIS

Section d'Application des Traceurs, Commissariat à l'Énergie Atomique, 17 Rue des Martyrs, F-38054 Grenoble Cedex 09, France

e-mail : n.courtois@brgm.fr

C. GRENIER, P. MAUGIS, E. MOUCHE

DRN/DMT/SMT/MTMS, CEA/Saclay, F-91191 Gif-sur-Yvette Cedex, France

C. de FOUQUET, P. GOBLET & E. LEDOUX

Ecole des Mines de Paris, 35 Rue Saint-Honoré, F-77305 Fontainebleau Cedex, France

Abstract Dispersion in aquifers is dominated by the spatial structure of the hydraulic conductivity field. The aim of the study is to characterize the dispersive properties of a heterogeneous aquifer located near Grenoble, France, through two approaches both based on the use of experimental tracing data: a deterministic approach, interpretation of field scale natural gradient tracer tests; and a statistical approach, the geostatistical study of the spatial structure of the experimental hydraulic conductivity field, followed by the spatial moment analysis of stochastic particle trajectories. With the choice of exponential variograms, the simulated longitudinal dispersivity fits quite well to the experimental one, and reaches an asymptotic limit of 6 m after a 50 m travel distance, say about ten correlation lengths, which accords with the stochastic theories.

INTRODUCTION AND SITE PRESENTATION

The field site is located near Grenoble (France), at the confluence of the rivers Drac and Isère. The aquifer is formed by a 30 m thick sequence of alluvial sediments, mostly composed of coarse gravel deposits, with inclusions of sand and clay lenses. It is underlain by a clay formation deposited in an ancient lake.

Spreading of a plume in such an aquifer is mainly controlled by the spatial structure of the hydraulic conductivity field, and by the presence of preferential channels which may correspond to ancient river channels. Classically, dispersion phenomenon in aquifers are supposed to be well described by the following equation:

$$\omega \frac{\partial C(\bar{x}, t)}{\partial t} = \bar{\nabla} \cdot (\bar{D} \cdot \bar{\nabla} C(\bar{x}, t)) - \bar{\nabla} \cdot (\bar{U} \cdot C(\bar{x}, t)) \quad (1)$$

with ω the effective porosity, $C(\bar{x}, t)$ the concentration at point \bar{x} and time t , \bar{U} the Darcyian velocity, and \bar{D} the dispersion tensor. The aim of the study is to characterize this dispersion tensor.

* Present address: BRGM, 1039 Rue de Pinville, F-34000 Montpellier, France

RESULTS OF THE NATURAL GRADIENT TRACER TESTS

The first approach to dispersion is the interpretation of natural gradient field-scale tracer tests. The experimental test site includes 17, 15 m deep fully-penetrating wells. The maximum extent is about 45 m along the main flow direction. Four tracer tests were conducted on the experimental site, with distances between injection and recovery wells ranging from 3 to 45 m.

Fluorescent tracers were injected, and their migration monitored in the recovery wells by sampling the depth-averaged concentration. Assuming that the flow is unidirectional in the x direction, the convection–dispersion equation (1) takes the following two-dimensional form:

$$\omega \frac{\partial C(x, y, t)}{\partial t} = D_L \frac{\partial^2 C(x, y, t)}{\partial x^2} + D_T \frac{\partial^2 C(x, y, t)}{\partial y^2} - U \frac{\partial C(x, y, t)}{\partial x} \quad (2)$$

with $C(x, y, t)$ the tracer concentration, U the mean Darcyian velocity in the x direction, D_L and D_T respectively the longitudinal and horizontal transverse components of the dispersion tensor. Neglecting molecular diffusion, the coefficients of dispersion can be expressed as:

$$D_L = \alpha_L U \quad D_T = \alpha_T U \quad (3)$$

with α_L and α_T respectively the longitudinal and horizontal transverse dispersivities.

Figure 1 shows the breakthrough curves obtained in two lines of wells, perpendicular to the main flow direction, and located at 6 and 45 m from the injection well. Longitudinal dispersion can be seen by comparing the arrival time distributions, and the ratios of peak concentration, between the two lines of wells. Transverse dispersion can be seen in the ratios of peak concentration in a given line.

For instantaneous injection of tracer (mass Δm) in an aquifer with parallel flow in two dimensions, the solution of equation (2) is given by Bear (1979):

$$C(x, y, t) = \frac{\Delta m / \omega}{4\pi t \sqrt{D_L D_T} / \omega^2} \exp\left(-\frac{(x - Ut/\omega)^2}{4D_L t/\omega} - \frac{y^2}{4D_T t/\omega}\right) \quad (4)$$

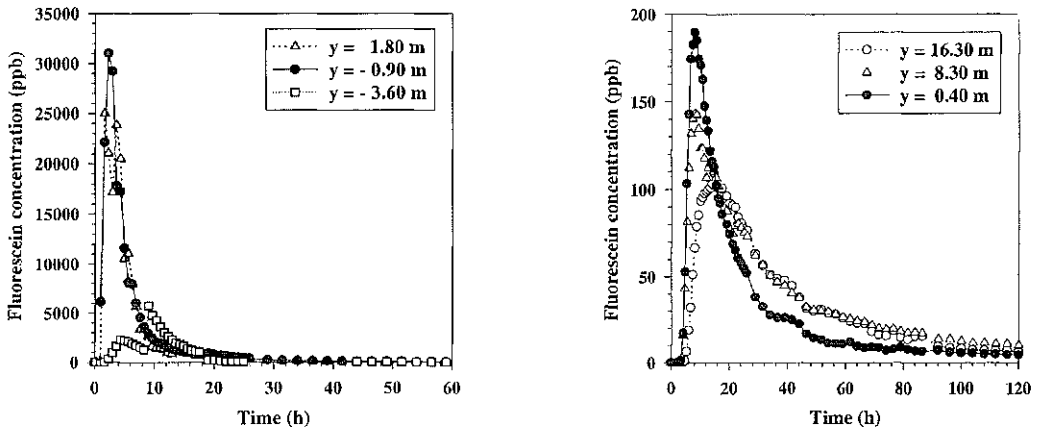


Fig. 1 Tracer breakthrough curves in two lines of wells located at $x = 6$ m (left) and $x = 45$ m (right) of the injection well.

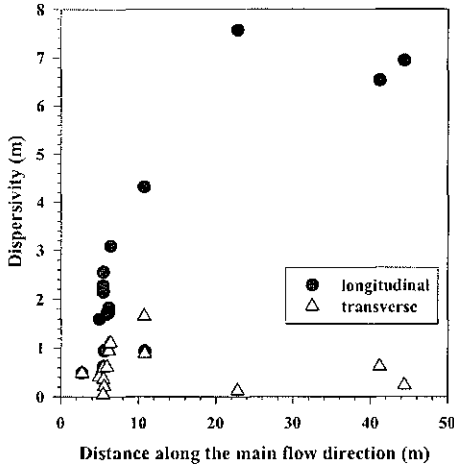


Fig. 2 Dispersivities calculated from field-scale tracer experiments.

Pore velocity (defined as U/ω) and dispersivities (Fig. 2) are estimated from the fit of equation (4) to the experimental breakthrough curves.

Longitudinal dispersivities tend to increase with the experimental distance, ranging from 0.50 to 7 m for travel distances ranging from 3 to 45 m. The question is whether an asymptotic limit of longitudinal dispersivity exists, and can be reached in the 45 m scale field tracer experiments.

Note that tracer recovery rates are small (from 20% to less than 1% for 3 to 45 m travel distance), and that the quality adjustment of equation (4) on the experimental curves decreases with travel distance, so the given dispersivity values remain numerical estimations. However, tracer tests are a practical and direct technique for field scale dispersion studies.

GEOSTATISTICAL ANALYSIS OF THE CONDUCTIVITY FIELD

The vertical distribution of the horizontal groundwater flow Q_h was measured in boreholes by the dilution method: a small amount of fluorescent tracer was injected instantaneously between packers and is diluted by the groundwater flow through this isolated volume V_b . This measurement method can be modelled as the combination of simple flow structures: piston-like flow and mixed flow-through reactors, which leads to an analytical expression of the tracer concentration vs time. For the study, we adopt however, an approximate solution, assuming that the isolated volume behaves like a unique mixed flow-through reactor. Q_h was then estimated from the fit of the exponential solution $C(t) = C_0 \exp(-t/(V_b/Q_h))$ on the end of the experimental dilution curves. Hydraulic conductivity K_h is then deduced from Q_h through Darcy's equation, assuming a 3‰ average hydraulic gradient on the site.

Such vertical profiles of one-metre averaged hydraulic conductivities are conducted in wells to lead to 185 values for the entire site. Figure 3 shows the depth profile of horizontal Darcyian velocity in two wells. Horizontal and vertical contrasts are clearly apparent despite the one-metre averaging.

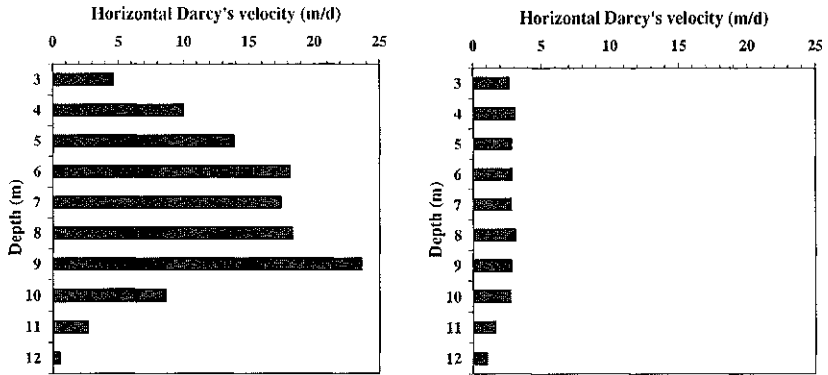


Fig. 3 Depth profile of horizontal Darcy's velocity in two wells 3 m away.

Figure 4, left, shows that the distribution of hydraulic conductivity approaches the lognormal one calculated with the experimental mean and variance of $\ln K_h$ values: $m_{\ln K} = -4.08$, and $\sigma_{\ln K}^2 = 1.21$. It is assumed to be lognormal in the study.

The spatial correlation of hydraulic conductivity field is described by variograms calculated in the horizontal and vertical directions, and computed as:

$$\gamma(h) = \frac{1}{2N(h)} \sum_{i=1}^{N(h)} (\ln K_h(x_i + h) - \ln K_h(x_i))^2 \tag{5}$$

with h the separation distance, x_i the location, and $N(h)$ the number of data pairs.

The horizontal experimental variogram (Fig. 4, right) increases regularly up to 8 m, then shows oscillations which may be partly explained by the decrease in number of data pairs with separation distance, and partly by the spatial heterogeneity of the field.

The choice of the exponential model $\gamma(h) = S \exp(-h/\lambda)$ to fit the variograms, leads to the following parameters: $S = \sigma_{\ln K}^2 = 1.21$, $\lambda_h = 5$ m, and $\lambda_v = 4.30$ m, with λ_h and λ_v respectively the horizontal and vertical correlation lengths.

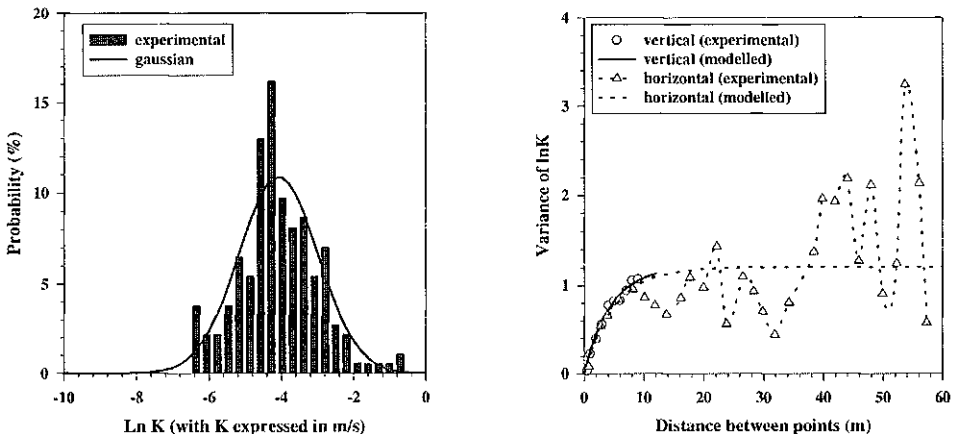


Fig. 4 Left: Histogram of $\ln K$ compared with a Gaussian one. Right: Horizontal and vertical variograms, experimental and modelled.

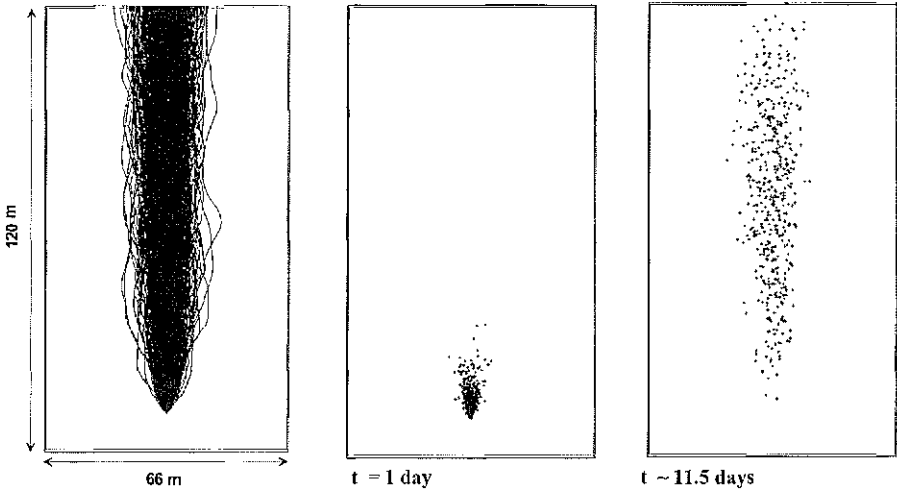


Fig. 5 Left: horizontal projection of 480 particles trajectories. Middle and right: particles' positions respectively at 1 and 11.5 days.

The question is whether the spatial law chosen to describe the hydraulic conductivity field is able to explain the dispersion phenomenon observed on the site.

STOCHASTIC MODELLING OF FLOW AND TRANSPORT

Three-dimensional stochastic hydraulic conductivity fields following the chosen spatial law are generated on a 1 m mesh regular grid, using the geostatistical software ISATIS (École des Mines de Paris). The dimensions of the grid are 120 × 66 × 50 m, which correspond about to (24λ_h) × (13λ_h) × (10λ_h). These fields are then incorporated into the finite elements code CASTEM2000 (CEA), to lead to the associated flow fields. The transport is modelled by particle-tracking and Monte-Carlo techniques.

Figure 5 shows the horizontal projection of 480 stochastic trajectories (with average hydraulic gradient along the x₁ axis), and particles positions after 1 and 11.5 days. Dispersion can be seen in the spreading of their arrival positions.

As a random variable, the particle's position $\vec{X}(t)$ is the sum of a statistical mean $\langle \vec{X}(t) \rangle$, linked to the mean velocity, and of a fluctuation term $\tilde{\vec{x}}(t)$, linked to the spatial structure of the flow field. Spatial second moments $(X_{ij})_{i,j=1,2,3}$, dispersion coefficients $(D_{ij})_{i,j=1,2,3}$, and macrodispersivities $(A_{ij})_{i,j=1,2,3}$ are defined by the spatial distribution of particles:

$$X_{ij}(t) = \langle \tilde{x}_i(t) \cdot \tilde{x}_j(t) \rangle, \quad D_{ij}(t) = \frac{1}{2} \cdot \frac{dX_{ij}(t)}{dt}, \quad A_{ij}(t) = \frac{1}{2} \cdot \frac{\partial X_{ij}(t)}{\partial X_1(t)} \tag{6}$$

The longitudinal second moment $X_{11}(t)$ (Fig. 6, left) along the main axis is much larger than the transverse ones, and shows a linear trend with time. After 300 h, more than 50% of particles have left the calculation grid, so the statistical result is no

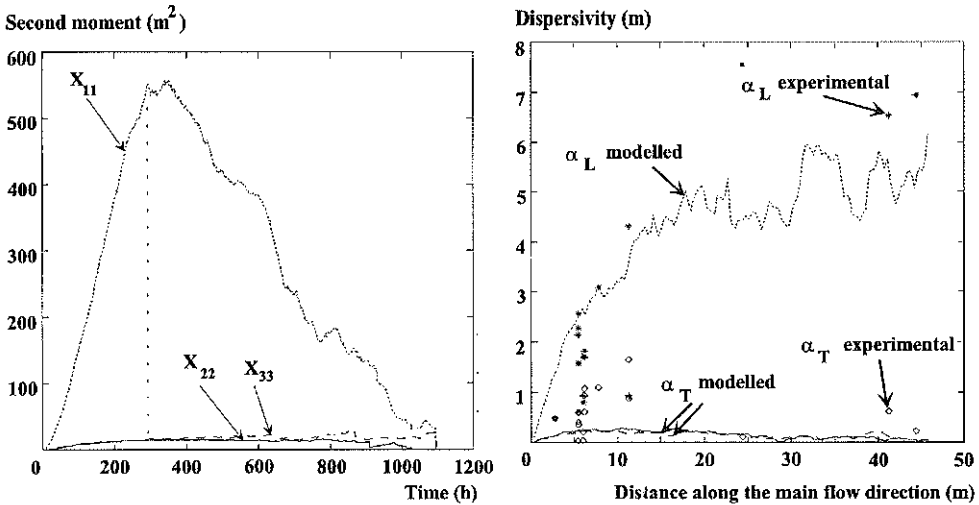


Fig. 6 Left: Second moments calculated with 480 particles trajectories. Right: Simulated macrodispersivities compared to the experimental ones.

longer valid. Longitudinal and transverse macrodispersivities calculated from equation (6) are plotted vs distance along the main flow direction (Fig. 6, right), to be compared to those deduced from tracer experiment (Fig. 2). The comparison is quite good: the rough estimate is well represented, as well as the increase of longitudinal dispersivity with distance. At 50 m, i.e. at $(10 \times \lambda_h)$ -travel distance, the simulated longitudinal dispersivity seems to reach an asymptotic value close to 6 m. This value matches with the theoretic asymptotic value A_∞ given by Dagan (1989), namely $A_\infty = \sigma_{\ln K}^2 \cdot \lambda_h$, with $\sigma_{\ln K}^2 = 1.21$, and $\lambda_h = 5$ m.

CONCLUSION

The quite good agreement between experimental and simulated dispersivities seems to show that the spatial structure of hydraulic conductivity field we underlined is able to explain the dispersion phenomenon in this aquifer. Some uncertainties remain, like adjustment on tracer breakthrough curves, precision of the experimental measure of hydraulic conductivity, and choice of variogram model. However, these two methods could be complementary on experimental sites sufficiently equipped.

Acknowledgements This work was funded and supported by the Section d'Application des Traceurs of the Commissariat à l'Énergie Atomique, Grenoble.

REFERENCES

- Bear, J. (1979) *Hydraulics of Groundwater*. McGraw-Hill, Inc., New York, USA.
 Courtois, N. (1999) Caractérisation de la dispersion en aquifère hétérogène par méthodes de traçage et modélisation stochastique. Thesis in Quantitative Hydrology and Hydrogeology, Ecole des Mines de Paris, Paris (to be edited).
 Dagan, G. (1989) *Flow and Transport in Porous Formations*. Springer-Verlag, Berlin, Germany.